ACS APPLIED MATERIALS & INTERFACES

Research Article

www.acsami.org

Microwave-Assisted Synthesis of High-Voltage Nanostructured $LiMn_{1.5}Ni_{0.5}O_4$ Spinel: Tuning the Mn^{3+} Content and Electrochemical Performance

Charl J. Jafta,[†,‡] Mkhulu K. Mathe,[†] Ncholu Manyala,[‡] Wiets D. Roos,[§] and Kenneth I. Ozoemena*[,†,⊥]

[†]Energy Materials, Materials Science and Manufacturing, Council for Scientific & Industrial Research (CSIR), Pretoria 0001, South Africa

[‡]Department of Physics, Institute of Applied Materials, SARChI Chair in Carbon Technology and Materials, University of Pretoria, Pretoria 0002, South Africa

[§]Department of Physics, University of the Free State, Bloemfontein, Bloemfontein 9300, South Africa

[⊥]Department of Chemistry, University of Pretoria, Pretoria 0002, South Africa

Supporting Information

ABSTRACT: The $LiMn_{1.5}Ni_{0.5}O_4$ spinel is an important lithium ion battery cathode material that has continued to receive major research attention because of its high operating voltage (~4.8 V). This study interrogates the impact of microwave irradiation on the Mn^{3+} concentration and electrochemistry of the $LiMn_{1.5}Ni_{0.5}O_4$ spinel. It is shown that microwave is capable of tuning the Mn^{3+} content of the spinel for enhanced electrochemical performance (high capacity, high capacity retention, excellent rate capability, and fast Li^+ insertion/extraction kinetics). This finding promises to revolutionize the application of microwave irradiation for improved performance of the $LiMn_{1.5}Ni_{0.5}O_4$ spinel, especially in high rate applications.

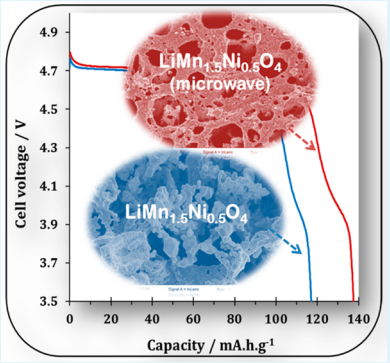

KEYWORDS: *$LiMn_{1.5}Ni_{0.5}O_4$, Pechini method, microwave irradiation, Mn^{3+} concentration, XPS, electrochemistry*

INTRODUCTION

Lithium-ion batteries (LIBs) have been described as the next generation of energy-storage devices for a variety of everyday applications such as electric vehicles, laptop computers, cell phones, etc. $LiMn_2O_4$ has received considerable attention as a cathode material for lithium-ion batteries as it is a low-cost and eco-friendly cathode material that can replace $LiCoO_2$, which is expensive and toxic.[1,2] Considering that $LiMn_2O_4$ has a relatively low operating voltage and suffers from capacity loss during cycling, the Mn site in $LiMn_2O_4$ has been substituted by various cations such as Co, Cr, Al, etc.[3−5] The spinel cathode material, $LiMn_{1.5}Ni_{0.5}O_4$, is considered an advanced LIB material and has been receiving major research attention because of its high operating voltage (~4.8 V) and the high intrinsic rate capability.[6] Because of this high operating voltage, the $LiMn_{1.5}Ni_{0.5}O_4$ full cells are shown to have an average (operating) voltage of ~3.4 V with an appropriate anode.[1] Despite its many advantages, $LiMn_{1.5}Ni_{0.5}O_4$ still encounters many obstacles for high-rate applications. It is very difficult to synthesize a pure and stoichiometric $Li_{1-x}[Ni_{0.5}Mn_{1.5}]O_4$ spinel as $Li_yNi_{1-y}O$ (impurity) appears as a second phase, negatively impacting the electrochemical behavior.[6,7]

$LiMn_{1.5}Ni_{0.5}O_4$ has two different crystal structures; (i) the stoichiometric ordered, composed only of Mn^{4+}, and (ii) the nonstoichiometric disordered, face-centered cubic structure ($Fd3m$) composed of Mn^{3+} and Mn^{4+}. The ordered phase ($LiNi_{0.5}Mn_{1.5}O_4$) is a primitive simple cubic structure ($P4_332$) in which Ni, Mn, and Li atoms respectively occupy the 4a, 12d, and 8c sites, whereas the O atoms reside in the 8c and 24e sites. The nonstoichiometric ($LiNi_{0.5}Mn_{1.5}O_{4-\delta}$) is a face-centered cubic structure ($Fd3m$) where Ni and Mn atoms are randomly distributed in the 16d sites, whereas Li and O occupy 8a tetrahedral sites and 32e sites, respectively.[8] It has been well-established that the preparation of either of the phases is determined by the annealing temperatures, ordered spinel at T = 700 °C and disordered spinel at T > 700 °C[9] (eq 1)[10−12]

$$LiMn_{1.5}Ni_{0.5}O_4 \leftrightarrow \alpha Li_xNi_{1-x}O + \beta LiMn_{1.5+y}Ni_{0.5-y}O_{4-x} + \gamma O_2 \ (T > 700°C) \quad (1)$$

The electrochemical performance of this spinel as a cathode material for lithium ion battery is intricately linked to the (i) presence of Mn^{3+} ions and/or the degree of disorder, (ii) doping/substitution with cations, and (iii) presence of

Received: May 19, 2013
Accepted: July 15, 2013
Published: July 15, 2013

   dx.doi.org/10.1021/am401894t | ACS Appl. Mater. Interfaces 2013, 5, 7592−7598

$Li_yNi_{1-y}O$ impurity. These factors explain why it still remains a huge challenge to correlate synthesis, structure and performance of this spinel material. The electrochemical performance of the disordered spinel is better than the ordered one mainly because of the enhanced Li^+ diffusion coefficient in the former. The formation of the disordered spinel is usually accompanied with the $Li_xNi_{1-y}O$ phase that lowers the obtainable capacity. To maintain charge neutrality in the disordered spinel (as a result of the loss of oxygen) part of the inactive Mn^{4+} ions are reduced to Mn^{3+} ions. The redox-active Mn^{3+} improves the spinel electronic conductivity, and gives a small signature peak plateau around 4 V. Higher Mn^{3+} ion content delivers a better discharge capacity at higher charge/discharge rates because of the improved electronic conductivity. However, a high concentration of Mn^{3+} would lead to disproportionation reactions that produce soluble Mn^{2+} in the electrolyte, which may cause severe capacity fading.[13,14] In a nutshell, if every Mn ion in the spinel is maintained at the 4+ state, we will only obtain a stoichiometrically ordered $LiNi_{0.5}Mn_{1.5}O_4$, an undesirable situation that may conspire against the fast Li^+ transportation. It is understandable therefore why the amount of Mn^{3+} ions is considered quite critical in determining the electrochemical performances of the spinel. In a recent report, Xiao et al.[13] elegantly showed that the concentration of Mn^{3+} ions in the spinel lattice is controlled by combining postsynthesis annealing and partially substituting Ni^{2+} with Cr^{2+}. In summarizing their findings, the authors concluded that the "comparison of the electrochemical performances of spinels with different Mn^{3+} contents demonstrates that careful control of the amount of Mn^{3+} ions and, thus, the disordered phase, is the key for synthesis of high-performance spinel and provides valuable clues for understanding the structure−property relationships in energy materials". To our knowledge, there are four reported methods for controlling the Mn^{3+} content in $LiNi_{0.5}Mn_{1.5}O_4$; (i) careful control of the cooling rate after high-temperature calcination;[14] (ii) partial substitution of Ni and/or Mn with elements such as Co, Al, Ti, Fe, Cr, Ru, or Mg;[6,13,15−18] (iii) combined postsynthesis annealing and partial substitution of Ni with Cr;[13] and (iv) long-hour acidic treatment.[19]

In this report, we introduce microwave-assisted synthesis as an elegant strategy to control the Mn^{3+} concentration (degree of disorder) and enhance the electrochemical performance of the $LiMn_{1.5}Ni_{0.5}O_4$ spinel material. Our proposed strategy is novel, simple, fast, and efficient, and importantly, promises to avoid many of the disadvantages associated with the state-of-the-art procedures such as (i) the use of energy-intensive and time-consuming careful controlling of the cooling rates after high-temperature calcination or the postsynthesis annealing; (ii) partial substitution of Ni or Mn with expensive metals (e.g., Ru), which may be toxic and environmentally unfriendly (e.g., Cr); and (iii) long-hour acid treatment.

The use of microwave irradiation to improve the performance of metallic materials has long been known,[20,21] and we recently showed how the microwave irradiation can be used to induce top-down nanostructuring for enhanced performance of core−shell palladium-based catalyst.[22] The microwave-enhanced chemical reaction is dependent upon the efficient interaction of molecules with the electromagnetic waves. Unlike the traditional heating process, the temperature of the surrounding in the microwave heating process is colder than that of the target sample (i.e., "in-core" heating, generated from within the sample). Although the mechanism of microwave-matter interaction is not perfectly understood, it is thought to occur via two physical phenomena, the electric (E) and magnetic (H) field vectors.[15]

EXPERIMENTAL SECTION

The $LiMn_{1.5}Ni_{0.5}O_4$ was prepared by a one-step powder-forming, Pechini-modified method involving the use of citric acid (CA), ethylene glycol (EG), and nitrate salts.[4,7] The reducing agent, CA (dissolved in deionized water) and EG was mixed in the ratio 1:4 (CA:EG) and heated at 90 °C while being stirred constantly for 30 min. Stoichiometric amounts of $LiNO_3$, $Ni(NO_3)_2{\cdot}6H_2O$ and $Mn(NO_3)_2{\cdot}4H_2O$ were dissolved in deionized water and introduced dropwise to the CA/EG solution. After heating the resultant solution to and maintaining it at 90 °C with constant stirring, the viscosity of the solution increased constantly because of evaporation of the water; the viscous solution subsequently dehydrated into a gel. The gel was kept at a temperature of 90 °C until the gel spontaneously burnt (typically about 30 min after the salt-containing solution was added to the reducing agent) to form the desired powder. The powder was preheated at 500 °C for 6 h to get rid of the carbonaneous materials, and then annealed at 700 or 800 °C for 8 h (herein referred to as LMN-700 or LMN-800, respectively). To study the impact of microwave irradiation, two batches of the preheated powder at 500 °C were subjected to microwave irradiation (using the Anton Paar Multiwave 3000 system, λ = 0.12236 m) at 600 W for 15 min, where the temperature of the samples reached a maximum of 60 °C (measured with an infrared thermometer, which is approximately 5 cm away from the bottom of the vessel containing the powders), and then annealed at 700 or 800 °C for 8 h (herein referred to as LMN-700-mic or LMN-800-mic, respectively).

The structural characterization was done by XRD using a Bruker AXS D8 ADVANCE X-ray Diffractometer with Ni-filtered Cu K_α radiation (λ = 1.5406 Å) for the LMN-700/LMN-700-mic and a PANalytical X′pert Pro Powder Diffractometer with Fe-filtered Co K_α radiation (λ = 1.7890 Å) for the LMN-800/LMN-800-mic. The scanning speed was 0.02° per step with a dwell time of 5 s for all samples. The LMN-700/LMN-700-mic and LMN-800/LMN-800-mic powders were mounted in a PHI 5400 ESCA and PHI 5000 Versaprobe−Scanning ESCA Microprobe vacuum chambers with base pressures $\leq 1 \times 10^{-8}$ Torr. X-ray Photoelectron Spectroscopy (XPS) was performed for LMN-700/LMN-700-mic and LMN-800/LMN-800-mic using a nonmonochromatic aluminum (Al) K_α source (1486.6 eV) and an Al monochromatic K_α source (1486.6 eV), respectively. The XPS data analysis was performed with the XPS Peak 4.1 program and a Shirley function was used to subtract the background.

Electrochemical measurements were performed in a two-electrode coin cell (LIR-2032) assembled with the LMN materials as the positive electrode and lithium metal foil as the negative electrode using a MACCOR series 4000 tester. The cathodes were prepared by coating the slurry of a mixture composed of 80% active material, 10% acetylene black, and 10% polyvinylidene fluoride onto cleaned and polished aluminum foil, with active mass loading of ∼2.5 mg. Subsequently, the materials were dried at 90 °C under vacuum ($\sim 1 \times 10^{-1}$ Torr) for 24 h. The cells were assembled in an argon-filled MBraun glovebox (O_2, H_2O < 0.5 ppm). The electrolyte was 1 M $LiPF_6$ in a mixture of 1:1 (v/v) EC:DMC. A polypropylene film (Cellgard 2300) was used as the separator.

RESULTS AND DISCUSSION

Figure 1 shows typical FESEM images of (a) LMN-800 and (b) LMN-800-mic, the latter depicting a spider weblike layered morphology made up of interconnected primary crystallites with hierarchical pores. The difference in the morphologies is due to the microwave irradiation that changes the growth kinetics. The LMN-800 sizes ranged between ∼50 and 200 nm and LMN-800-mic between ∼50 and 100 nm. The LMN-700 particle sizes ranged between ∼100 and 200 nm, whereas those of the LMN-700-mic ranged between ∼50 and 100 nm (Figure

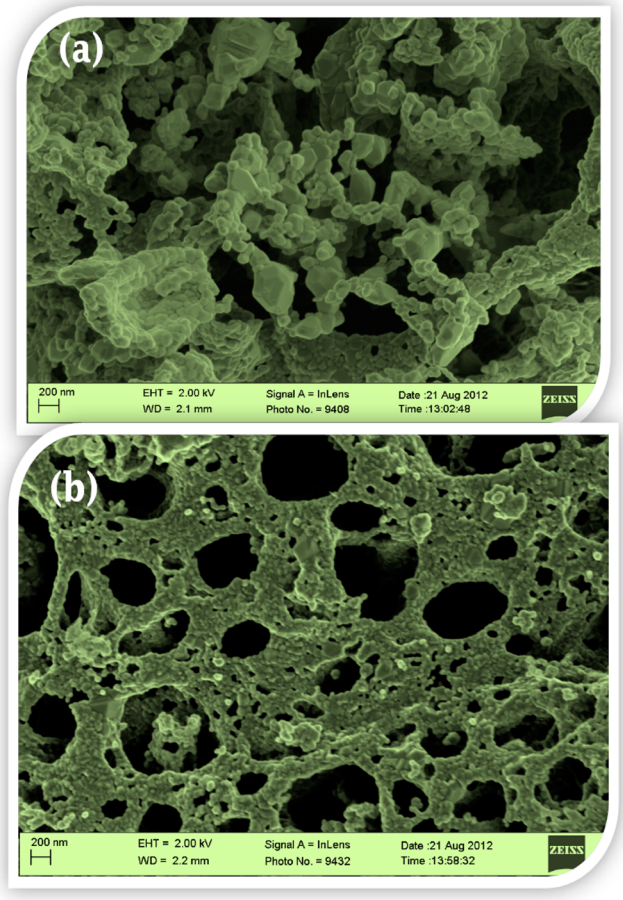

Figure 1. Typical FE-SEM images of (a) LMN-800 and (b) LMN-800-mic. Scale bar = 200 nm.

SI 1 in the Supporting Information). Thus, the particle sizes of the microwave-treated samples are smaller than the bare samples, suggesting that upon microwave irradiation, crystallization of the spinel is almost complete thus making further particle growth via annealing (at 700 or 800 °C) slow compared to the bare samples.

The powder XRD patterns (Figures 2 and Figure SI 2 in the Supporting Information) are characteristic of the cubic spinel structures with the microwave-treated samples showing sharper

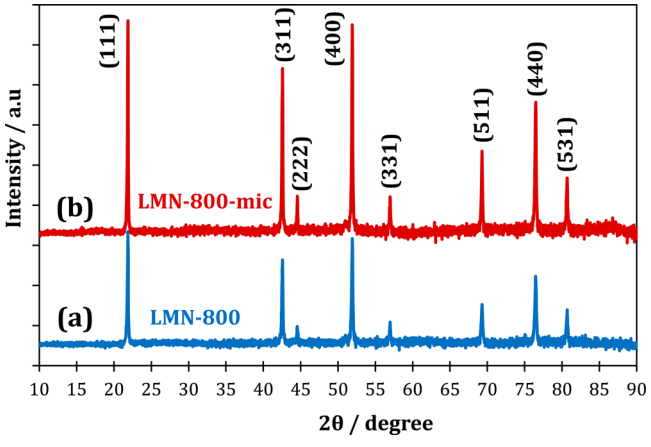

Figure 2. Typical powder X-ray diffraction patterns of (a) LMN-800 and (b) LMN-800-mic.

diffraction peaks than the bare samples, meaning that microwave irradiation enhanced crystallinity in the spinel. The impurity phase is virtually nonexistent in the materials. The lattice parameters (a-value/Å and unit cell volume/Å^3) were calculated as 8.153 Å and 541.907 Å^3 for the LMN-700; 8.160 Å and 543.170 Å^3 for the LMN-700-mic; 8.180 Å and 547.417 Å^3 for the LMN-800; 8.179 Å and 547.109 Å^3 for the LMN-800-mic. These values are comparable to values in the literature.[23]

From the XRD patterns of the LMN-700 and LMN-700-mic, the latter shows preferential crystal growth according the (111) reflection (Figure SI 2 in the Supporting Information), which may be ascribed to the microwave irradiation that changes the crystal growth kinetics. The slight increase in the lattice parameters for the pristine 800 sample compared to its 700 counterpart further proves that the 800 sample is Mn^{3+}-enriched (disordered phase). The increase in the lattice parameter for the LMN-700-mic indicates the creation of some oxygen vacancies in the spinel structure following the microwave irradiation process which causes some Mn^{4+} ions to be converted to Mn^{3+} due to charge compensation.[13,24] On the other hand, the lattice parameters for the LMN-800 and LMN-800-mic suggests a slight decrease in the oxygen vacancies for the microwave-irradiated disordered material. This is interesting as it suggests that at the experimental conditions employed in this work, microwave irradiation simply adjusts the Mn^{3+} content to a lower value. As we will see later, these adjustments of the Mn^{3+}/Mn^{4+} ratios (or oxygen vacancy concentration) have profound effects on the electrochemical properties of the spinel as a cathode material for lithium ion battery.

During the microwave treatment that follows the preheating process, the microwave energy exerted onto the sample penetrates the sample and oxygen vacancies are created. Then the sample is annealed at a temperature lower than the onset temperature to create oxygen vacancies (T = 700 °C),[9] which will cause no further increase in the oxygen vacancies in the lattice. Therefore, it is seen that with the microwave treatment, oxygen vacancies are created and with the annealing process at T = 700 °C it remains in the lattice. When the LMN-800 is treated with microwave radiation, oxygen vacancies are created in the lattice. When annealed at 800 °C the oxygen-deficient cathode material will allow oxygen back into the lattice to achieve an equilibrium concentration. Also, the so-called specific or nonthermal microwave effects can still still play a role, though this is still a subject of some controversy.[25,26]

To determine the actual amounts of the Mn^{3+} and Mn^{4+} in the spinel, XPS experiments were performed for the powdered spinel samples. Figure 3 show the deconvoluted, detailed XPS of the Mn $2p_{3/2}$ peaks of the LMN-700/LMN-700-mic and LMN-800/LMN-800-mic samples. Two peaks (as marked) are attributed to Mn^{3+} and Mn^{4+} and another (in the LMN-700/LMN-700-mic spectra) to a Ni Auger peak. The binding energy peak positions corresponding to Mn^{4+} and Mn^{3+} are comparable with other binding energy values reported in literature.[27,28]

As shown in Table 1, the ratio of Mn^{3+} to Mn^{4+} (i.e., Mn^{3+}/Mn^{4+}) is 2.2 and 3.3 for the LMN-700 and LMN-700-mic, respectively. This increase in the Mn^{3+} content is in good agreement with the XRD data of the increased a-lattice parameter, further confirming that microwave irradiation causes oxygen deficiency causing the Mn^{4+} to be converted to Mn^{3+} in the ordered spinel. For the LMN-800 and LMN-800-mic, the Mn^{3+}/Mn^{4+} is 2.6 and 1.7, respectively. Again, this is in good

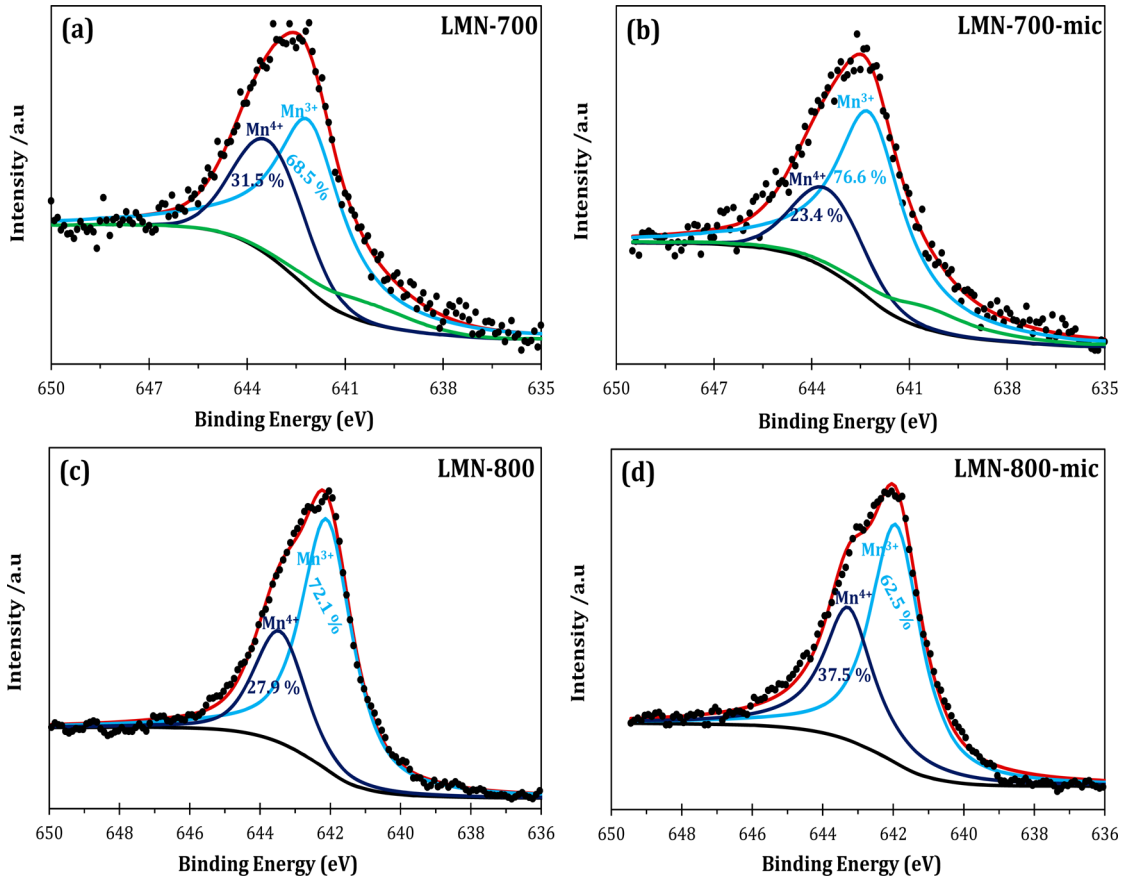

Figure 3. X-ray photoelectron spectra of the Mn $2p_{3/2}$ peak of (a) LMN-700, (b) LMN-700-mic, (c) LMN-800, and (d) LMN-700-mic.

Table 1. Mn $2p3_{/2}$ Peak Positions and Cation Distribution

	binding energy position (eV)		cation distribution		
sample	Mn^{4+}	Mn^{3+}	Mn^{4+} (%)	Mn^{3+} (%)	Mn^{3+}/Mn^{4+}
LMN-700	643.2	642.1	31.5	68.5	2.17
LMN-700-mic	643.4	642.2	23.4	76.6	3.27
LMN-800	643.4	642.1	27.9	72.1	2.58
LMN-800-mic	643.3	641.9	37.5	62.5	1.67

agreement with the XRD data that predicted a slight downward adjustment of the Mn^{3+} content of the disordered sample.

Figure 4 displays the cyclic voltammetric evolutions of LMN-700/LMN-700-mic and LMN-800/LMN-800-mic cathode materials, depicting the Li extraction/insertion behavior of the samples. The CVs of the bare and microwave-treated samples are significantly different, the latter showing better resolved and sharper peaks than the former. The difference in the peak-to-peak potential (ΔE_p) for the Ni^{2+}/Ni^{3+} redox couple is smaller for the LMN-700-mic (0.288 V vs Li/Li^+) than the LMN-700 (0.637 V vs Li/Li^+), a clear indication that the microwave-treated sample is more reversible with faster electrochemical kinetics than the bare samples. In addition, the Mn^{3+}/Mn^{4+} redox wave at 4 V is more defined than that of the bare samples. The peaks for the disordered spinel are more resolved with narrower ΔE_p than those of the ordered spinels. The ΔE_p for the nickel peaks, Ni^{2+}/Ni^{3+} (II/V or II′/V′) and Ni^{3+}/Ni^{4+} (III/IV or III′/IV′), are smaller (0.219 and 0.165 V) for the LMN-800-mic than the LMN-800 (0.371 and 0.287 V), meaning that the LMN-800-mic gives faster lithium extraction/insertion kinetics.

Figure 5 compares the first and 25th discharge profiles of LMN-700/LMN-700-mic and LMN-800/LMN-800-mic discharged at 0.1 C (14 mA g^{-1}). Unlike the materials obtained at 700 °C, the samples from 800 °C showed well-defined plateaus at 4 V due to the Mn^{3+}/Mn^{4+} redox couple, signature of 'disordered' spinel. In addition, the Ni^{2+}/Ni^{3+} and Ni^{3+}/Ni^{4+} redox couples of the disordered spinel are activated upon cycling, suggesting some structural changes induced by electrochemical cycling. The Mn^{3+}/Mn^{4+} peaks are well-defined in the 800 °C compared to the 700 °C samples. The capacity of the LMN-700 decreased from the first cycle (103 mAh/g) to the 25th cycle (96 mAh/g), which is typical of ordered spinel.[29] However, upon microwave treatment, the initial capacity of the LMN-700-mic (117 mAh/g) increased to 130 mA h/g at the 25th cycle. For the 800 °C samples, the initial cycles of the bare and the microwave-treated samples (105 and 125 mA h/g, respectively) increased upon cycling (117 and 138 mA h/g at the 25th cycle, respectively). This increase in capacity upon cycling could be atributed to the wetting process of the electrodes with the electrolytes prior to stabilization of the electrochemical reactions.[30] The higher performance of the LMN-800-mic over the bare sample suggests the intrinsic ability of microwave irradiation to adjust the Mn^{3+} concentration in the spinel for enhanced electrochemistry.

Next, we explored the cycle stability of the spinel samples at 50 repetitive cycles. This number of cycle was chosen as it provided enough information for the comparative studies, and also considering that other workers have used the same number[31] or even less[32] for the same LMN spinel. Figure 6 compares the cycle stability of the bare and microwave-treated

dx.doi.org/10.1021/am401894t | ACS Appl. Mater. Interfaces 2013, 5, 7592−7598

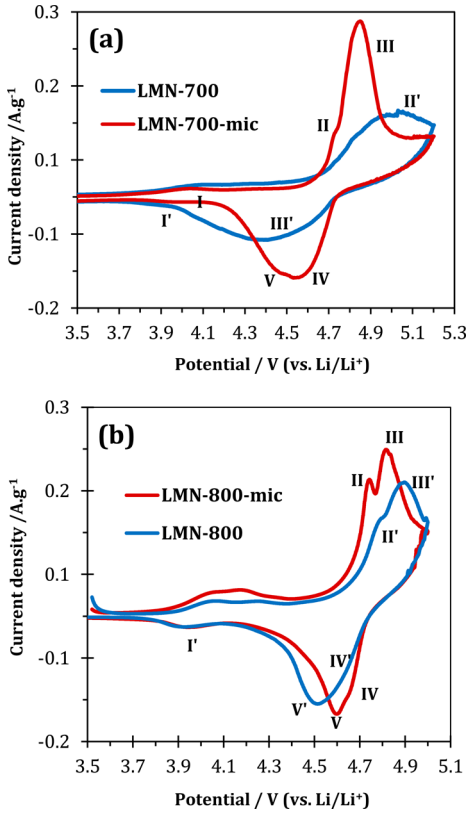

Figure 4. Representative cyclic voltammograms of (a) LMN-700/LMN-700-mic and (b) LMN-800/LMN-800-mic obtained at a scan rate of 0.1 mVs^{-1}.

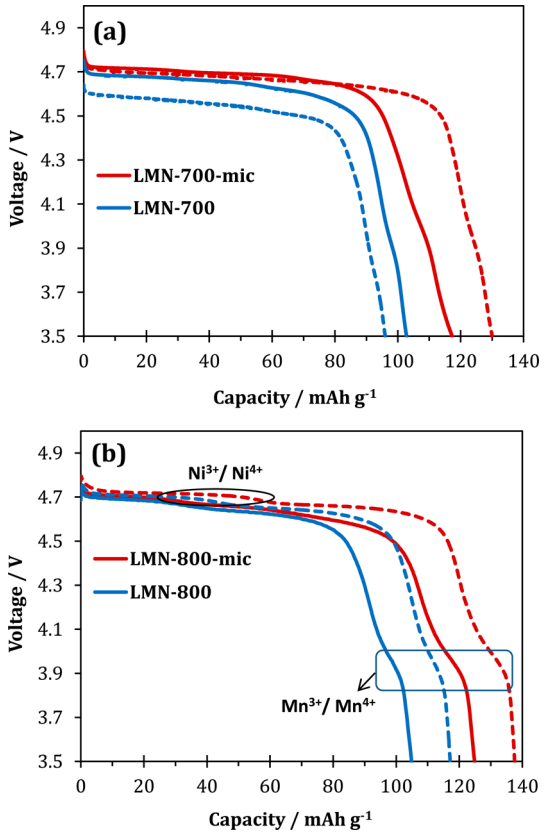

Figure 5. 1st (solid line) and 25th (broken line) discharge curves of LMN-800/LMN-800-mic at 0.1 C.

samples, which clearly proves that microwave irradiation improves the cyclability of the spinels (for both the ordered and disordered structures, with the latter benefitting the most). The extreme capacity fading for the 700 °C samples after the 25th cycle is related to the high amount of the nonconductive Mn^{4+} ions in the spinel. This fading behavior is consistent with LMN obtained at 700 °C regardless of the synthetic method or particle size.[12,31] It is interesting, however, to observe that microwave irradiation may serve as a viable strategy to improve the capacity retention for such LMN at 700 °C.

As indicated by Figure 7, the best performance is always obtained by the LMN-800-mic sample, with a capacity retention of ca.100% between the 10th and 50th cycle, compared to the capacity retentions of ∼97 and 84% for LMN-800 and LMN-700-mic, respectively. The excellent capacity retention of the LMN-800-mic may be partly due to the higher connectivity of the nanoparticles as seen in the FESEM pictures, and partly to the "appropriate" amount of Mn^{3+} induced by the microwave irradiation. In general, it is common knowledge that the LMN sample obtained at higher temperature (800 °C, disordered) shows better electrochemical performance than the 700 °C (ordered). Some of the reasons may be due to the better crystallinity and increased conductivity for the the Mn^{3+} compared to the Mn^{4+}.

For high-power applications, good rate capability is of utmost importance for any cathode materials for lithium-ion battery. In this study, the 800 °C samples were charged at 14 mA/g (0.1 C) and discharged between 70 mA/g (0.5 C) and 1400 mA/g (10 C). Figure 7 clearly proves that microwave treatment greatly enhances the rate capability of the spinel material. The high rate capability of the LMN-800-mic compared to the LMN-800 suggests that lithium-ion diffusion path length is shorter in the former than the latter. Our results are comparable and even superior to many LMN samples obtained by the Pechnini method[9,12] and other methods.[31,33] For example, at a high current density (e.g., 5 C), our LMN-800-mic recorded above 100 mAh/g, which compares with the values for the micrometer-sized carbon-coated LMN obtained by carbonization of sucrose at 850 °C, and even much better than the uncoated LMN sample that gave only about 70 mA h/g.[33]

Considering the high performance of the disordered LMN-800 and LMN-800-mic materials, further studies on their lithium diffusive properties were explored using the electrochemical impedance spectroscopy (spectra not shown) and employing the established equation[34]

$$D_{Li} = \left(\frac{2RT}{\sqrt{2}n^2F^2\sigma AC_{Li}}\right)^2 = \frac{2R^2T^2}{n^4F^4\sigma^2A^2C_{Li}^2} \quad (2)$$

where D_{Li} is the diffusion coefficient of lithium ions, R the gas constant, T the absolute temperature, A the geometric surface area of the cathode, F the Faraday constant, n the number of electrons transferred per molecule during oxidation and C_{Li} the lithium concentration in the cathode material. The Warburg factor, σ, is the obtained from the slope of the real impedance (Z') vs the reciprocal square root of the frequency in the low frequency region ($\omega^{-1/2}$) (Figure 8).[34] The estimated diffusion coefficients showed that the microwave treated sample is about an order of a magnitude (ca. 1.3×10^{-12} cm^2 s^{-1}) higher than the bare sample (ca. 2.7×10^{-13} cm^2s^{-1}). The D_{Li} values are in the same range found in the literature.[6,35]

dx.doi.org/10.1021/am401894t | ACS Appl. Mater. Interfaces 2013, 5, 7592−7598

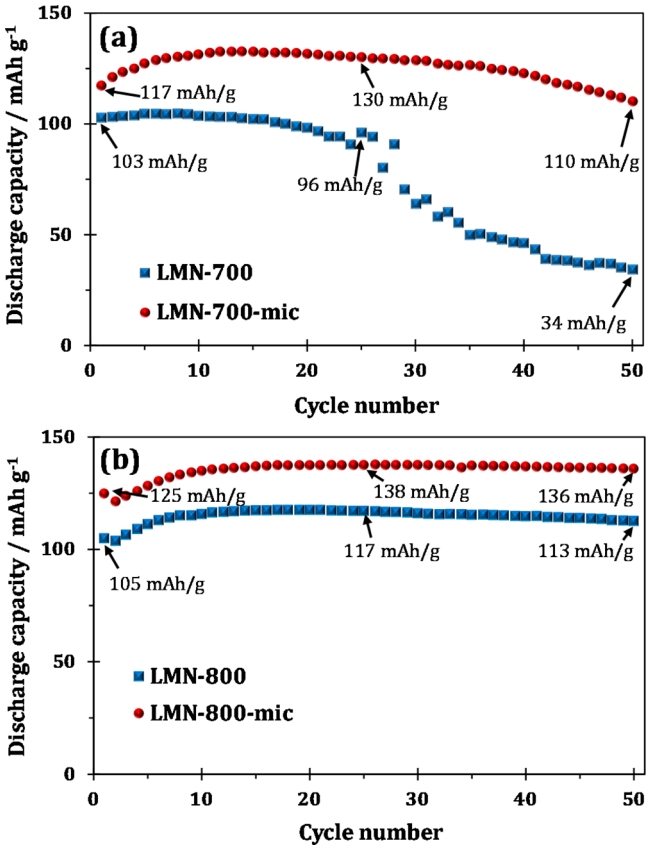

Figure 6. Cycle stability of (a) LMN-700/LMN-700-mic and (b) LMN-800/LMN-800-mic at 0.1*C*.

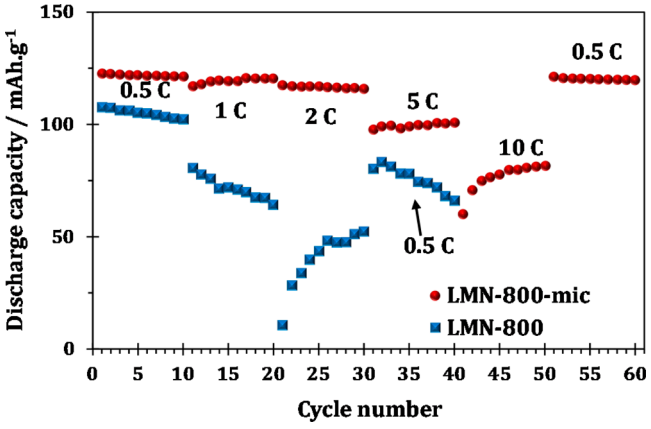

Figure 7. Typical rate capability plots for the LMN-800 and LMN-800-mic, charged at 0.1*C* but discharged at different rates, 0.5−10*C*.

CONCLUSIONS

This work has shown, for the first time, that microwave irradiation is capable of tuning the Mn^{3+} concentration (and hence the degree of disorder) for enhanced electrochemical performance (high capacity, high capacity retention, excellent rate capability, and fast Li^+ insertion/extraction kinetics) of the high-voltage $LiMn_{1.5}Ni_{0.5}O_4$ spinel cathode material for lithium ion battery. Indeed, this preliminary finding promises to revolutionize the application of $LiMn_{1.5}Ni_{0.5}O_4$ spinel for high rate applications. However, further studies toward micrometer-sized spinel, thermal stability, and scale-up will be needed.

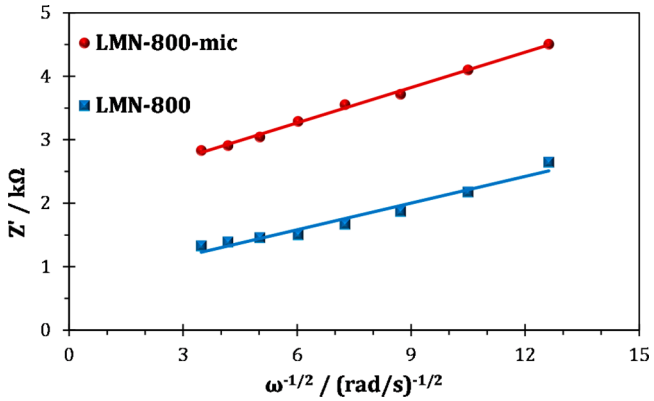

Figure 8. Plots of Z' vs $\omega^{-1/2}$ of LMN-800 and LMN-800-mic.

ASSOCIATED CONTENT

Supporting Information

FE-SEM images (Figure SI 1) and XRD patterns (Figure SI 2) of LMN-700 and LMN-700-mic. This material is available free of charge via the Internet at http://pubs.acs.org/.

AUTHOR INFORMATION

Corresponding Author

*E-mail: kozoemena@csir.co.za. Fax: +27 12 841 2135. Tel: +27 12 841 3664.

Notes

The authors declare no competing financial interest.

ACKNOWLEDGMENTS

This work was supported by the CSIR and DST/NRF nanotechnology flagship programme. C.J.J. thanks the CSIR for a PhD studentship.

REFERENCES

(1) Reddy, M. V.; Subba Rao, G. V.; Chowdari, B. V. R. *Chem. Rev.* **2013**, *113*, 5364−5457.
(2) Reddy, M. V.; Raju, M. J. S.; Sharma, N.; Quan, P. Y.; Nowshad, S. H.; Emmanuel, H. E.; Peterson, V. K.; Chowdari, B. V. R. *J. Electrochem. Soc.* **2011**, *158*, A1231−A1236.
(3) Sakunthala, A.; Reddy, M. V.; Selvasekarapandian, S.; Chowdari, B. V. R.; Selvin, P. C. *Electrochim. Acta* **2010**, *55*, 4441−4450.
(4) Reddy, M. V.; Sakunthala, A.; Pandian, S. S.; Chowdari, B. V. R. *J. Phys. Chem. C* **2013**, *117*, 9056−9064.
(5) Sigala, C.; Guyomard, D.; Verbaere, A.; Piffard, Y.; Tournoux, M. *Solid State Ionics* **1995**, *81*, 167−170.
(6) Liu, J.; Manthiram, A. *J. Phys. Chem. C* **2009**, *113*, 15073−15079.
(7) Liu, D.; Han, J.; Goodenough, J. B. *J. Power Sources* **2010**, *195*, 2918−2923.
(8) Kim, J. H.; Myung, S. -.; Yoon, C. S.; Kang, S. G.; Sun, Y. -. *Chem. Mater.* **2004**, *16*, 906−914.
(9) Kunduraci, M.; Al-Sharab, J. F.; Amatucci, G. G. *Chem. Mater.* **2006**, *18*, 3585−3592.
(10) Oh, S. H.; Chung, K. Y.; Jeon, S. H.; Kim, C. S.; Cho, W. I.; Cho, B. W. *J. Alloys Compd.* **2009**, *469*, 244−250.
(11) Wang, L.; Li, H.; Huang, X.; Baudrin, E. *Solid State Ionics* **2011**, *193*, 32−38.
(12) Kunduraci, M.; Amatucci, G. *J. Electrochem. Soc.* **2006**, *153*, A1345−A1352.
(13) Xiao, J.; Chen, X.; Sushko, P. V.; Sushko, M. L.; Kovarik, L.; Feng, J.; Deng, Z.; Zheng, J.; Graff, G. L.; Nie, Z.; Choi, D.; Liu, J.; Zhang, J.; Whittingham, M. S. *Adv. Mater.* **2012**, *24*, 2109−2116.
(14) Zheng, J.; Xiao, J.; Yu, X.; Kovarik, L.; Gu, M.; Omenya, F.; Chen, X.; Yang, X.; Liu, J.; Graff, G. L.; Whittingham, M. S.; Zhang, J. *Phys. Chem. Chem. Phys.* **2012**, *14*, 13515−13521.

(15) Ito, A.; Li, D.; Lee, Y.; Kobayakawa, K.; Sato, Y. *J. Power Sources* **2008**, *185*, 1429−1433.
(16) Locati, C.; Lafont, U.; Simonin, L.; Ooms, F.; Kelder, E. M. *J. Power Sources* **2007**, *174*, 847−851.
(17) Zhao, G.; Yang, Y.; Lin, Y.; Zeng, B.; Zhou, T.; Lin, Y.; Huang, Z. *2012 IEEE Asia-Pacific Power and Energy Engineering Conference (APPEEC)*; IEEE: Pisctaway, NJ, 2012; pp 1−5.
(18) Reddy, M. V.; Manoharan, S. S.; John, J.; Singh, B.; Subba Rao, G. V.; Chowdari, B. V. R. *J. Electrochem. Soc.* **2009**, *156*, A652−A660.
(19) Park, J. S.; Roh, K. C.; Lee, J.; Song, K.; Kim, Y.; Kang, Y. *J. Power Sources* **2013**, *230*, 138−142.
(20) Roy, R.; Peelamedu, R.; Hurtt, L.; Cheng, J.; Agrawal, D. *Mater. Res. Innov.* **2002**, *6*, 128−140.
(21) Nithya, C.; Thirunakaran, R.; Sivashanmugam, A.; Gopukumar, S. *ACS Appl. Mater. Interfaces* **2012**, *4*, 4040−4046.
(22) Fashedemi, O. O.; Julies, B.; Ozoemena, K. I. *Chem. Commun.* **2013**, *49*, 2034−2036.
(23) Reddy, M. V.; Cheng, H. Y.; Tham, J. H.; Yuan, C. Y.; Goh, H. L.; Chowdari, B. V. R. *Electrochim. Acta* **2012**, *62*, 269−275.
(24) Idemoto, Y.; Narai, H.; Koura, N. *J. Power Sources* **2003**, *119*−*121*, 125−129.
(25) Nüchter, M.; Ondruschka, B.; Bonrath, W.; Gum, A. *Green Chem.* **2004**, *6*, 128−141.
(26) de la Hoz, A.; Díaz-Ortiz, Á; Moreno, A. *Chem. Soc. Rev.* **2005**, *34*, 164−178.
(27) Wei, Y.; Yan, L.; Wang, C.; Xu, X.; Wu, F.; Chen, G. *J. Phys. Chem. B* **2004**, *108*, 18547−18551.
(28) Shaju, K. M.; Subba Rao, G. V.; Chowdari, B. V. R. *Electrochim. Acta* **2003**, *48*, 1505−1514.
(29) Shaju, K. M.; Bruce, P. G. *Dalton Trans.* **2008**, 5471−5475.
(30) Saint, J.; Best, A.; Hollenkamp, A.; Kerr, J.; Shin, J.; Doeff, M. *J. Electrochem. Soc.* **2008**, *155*, A172−A180.
(31) Dong, Y.; Wang, Z.; Qin, H.; Sui, X. *RSC Adv.* **2012**, *2*, 11988−11992.
(32) Hai, B.; Shukla, A. K.; Duncan, H.; Chen, G. *J. Mater. Chem. A* **2013**, *1*, 759−769.
(33) Yang, T.; Zhang, N.; Lang, Y.; Sun, K. *Electrochim. Acta* **2011**, *56*, 4058−4064.
(34) Jafta, C. J.; Ozoemena, K. I.; Mathe, M. K.; Roos, W. D. *Electrochim. Acta* **2012**, *85*, 411−422.
(35) Mohamedi, M.; Makino, M.; Dokko, K.; Itoh, T.; Uchida, I. *Electrochim. Acta* **2002**, *48*, 79−84.